

Numerical Simulation on Failure Characteristics of Inclined Soft Coal Strip Pillar

Sin Myong Nam*

Faculty of Mining Engineering, Kim Chaek University of Technology, Pyongyang, DPRK

*Corresponding author: Email: smn63312@star-co.net.kp

Summary

In the past, we determined the dimension of inclined coal strip pillars by using a general vertical pillar calculation method without considering pillar failure characteristics depending on the dip of a soft anthracite coal seam. In this paper, we suggest a method for determining the width of the inclined soft coal strip pillar that is left under the conditions of the caving coal mining or chamber coal mining suitable to the characteristics of dust coal seam and roof formations. The complete stress–strain curves for coal specimens were determined through laboratory tests, and using FLAC3D the failure characteristics and the bearing capacity of the inclined soft coal pillar were simulated. Through the numerical simulation and field observation, we proved that the failure characteristics of an inclined soft coal strip pillar are remarkably related to the dip of the coal pillar and since various kinds of inclined coal pillars left in the mining areas have been already failed, roof rock is supported on their residual strength.

Keywords: Soft anthracite coal; Coal strip pillar; Complete stress–strain curve; Numerical modeling; Failure strength

1. Introduction

Pillars in coal mines serve various purposes e.g. protection of gate roadways or entries, panel isolation to guard against spontaneous heating, protection of mine shafts and surface subsidence control. Traditionally, coal pillars are designed using conventional approaches, based on the principle that the strength of a pillar must be greater than the load imposed on it. A large number of coal pillar strength approaches proposed so far can be classified into four types: empirical, semi-empirical, statistical and analytical.

Various researchers [1~6] have conducted extensive field test and numerical simulations on coal pillars of different width-to-height ratios (w/h) for estimation of stress–strain behavior. The complete stress–strain curves of the coals that researchers have used in numerical modeling were obtained from coal samples with compressive strength of over 35MPa. However, the anthracite coal in our country has become dust to have compressive strength of less than 5MPa, so the bearing capacity of our coal pillars may not be estimated using the complete stress–strain curves suggested in [7~11].

With the aid of FLAC3D, the failure and residual strength of strip coal pillars with various dip angles are determined on the basis of the complete stress–strain curves of coal and they are compared with the field observation.

In the past, we determined the dimension of inclined coal strip pillars by using a general vertical pillar calculation method without consideration of pillar failure characteristics depending on the dip of a soft anthracite coal seam. The method suggested in this paper cannot be applied to the design of permanent water-proof coal pillars for rivers and faults, but can be applied to the determination of the level pillar width in the caving mining coal face or widths of interchamber pillars

and boundary pillars in chamber mining coal faces.

2. Numerical simulation

2.1. Determination of complete stress–strain curves of anthracite coal by tri-axial compressive test

We picked out samples from the area concerned in order to discover complete stress–strain characteristics of anthracite coal. The samples are processed to be 5cm in diameter, 10cm in height, 0.001 in the vertical degree and ± 0.03 in the parallel degree. The number of sample pieces at every stress level was set as 7 from the results of the preceding researches on tri-axial compressive testing of anthracite coal samples.

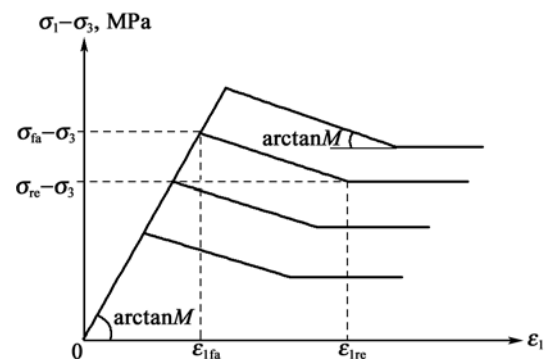


Figure 1. Elasto-plastic strain softening model of anthracite coal

In Fig. 1, σ_{1fa} and σ_{1re} are failure and residual strength, and ϵ_{1fa} and ϵ_{1re} are failure and residual strain depending on the lateral pressure σ_3 respectively.

Table 1. Failure and residual strength and strain characteristic magnitude depending on lateral pressure σ

Strength and strain values	Lateral pressure σ_3 , MPa						
	0	2.5	5	7.5	10.0	12.5	15.0
Failure strength σ_{1fa} , MPa	4.98	11.45	15.79	22.79	29.89	34.42	41.68
ϵ_{1fa}	0.009 3	0.011 8	0.014 6	0.024 2	0.026 1	0.027 2	0.032 7
Residual strength σ_{1re} , MPa	3.26	9.67	13.59	18.43	23.13	33.45	36.48
ϵ_{1re}	0.102	0.157	0.175	0.164	0.194	0.202	0.209

After inserting an enclosed sample into the hydraulic cylinder and ensuring hydrostatic pressure ($\sigma_1 = \sigma_2 = \sigma_3$) corresponding to the lateral pressure ($\sigma_2 = \sigma_3$), compressive load was given to it to change σ_1 , that is, equal tri-axial compressive ($\sigma_2 = \sigma_3$) test is used. The complete stress-strain characteristics of rock under the conditions of stereo stress state are denoted as the relation between stress density and strain density, which is shown in Fig. 1. In Fig. 1, σ_{1fa} and σ_{1re} are failure and residual strength and ε_{1fa} and ε_{1re} are failure and residual strain depending on lateral pressure σ_3 respectively.

2.2. Consideration of failure characteristics of inclined soft coal strip pillar

2.2.1. Failure characteristics of vertical soft coal strip pillar

The width of a strip coal pillar can be determined depending on rock pressure and its bearing capacity. Anthracite coal seams in our country are classified as follows according to their angles less than 25° accounts for 37.5%, 25~45° for 47.5% and larger than 45° for 15%. In case of mining such coal seams, various kinds of coal mining methods such as level caving method, sub-level caving method or chamber method and so on can be applied to retreating coal. In this case, coal pillars left, that is, level coal pillars, interchamber pillars and boundary pillars belong to an inclined strip coal pillar.

To compare the bearing capacity of a vertical pillar with that of an inclined pillar, the bearing capacity of the coal pillar was examined with an elasto-plastic strain softening model of coal using FLAC3D. The vertical stress acting to the coal pillar had estimated to be the weight of roof rock of 50~300m thick and the coal pillar was 4m in width and 4m in height. The coal pillar was simulated as a plane strain problem. Under such load condition, vertical pillars started to fail at the depth of 210m and completely failed at the depth of 215m. The failure state of the pillar is shown in Fig. 2.

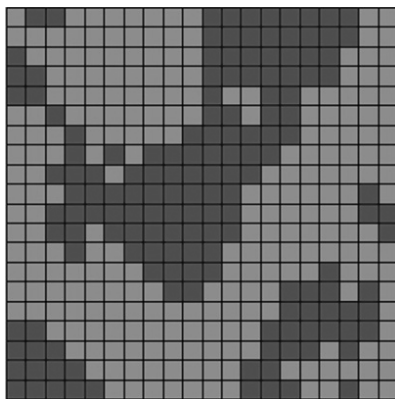


Figure 2. Failure state of coal pillar at the depth 215m

The complete stress-displacement curve of the coal pillar in this case is shown in Fig. 3.

In Fig. 3 above, the longitudinal axis denotes the vertical stress (unit: Pa) acting to the coal pillar and the transverse axis denotes the vertical displacement (unit: m). The axes in the figures below, which show the complete stress-strain curves of the coal pillar have the same meaning. In Fig. 3, the failure load and displacement coincide with the experimental data given in Table 1. After the coal pillar was completely failed at the depth of 215m, the residual strength of the coal pillar was about 15MPa.

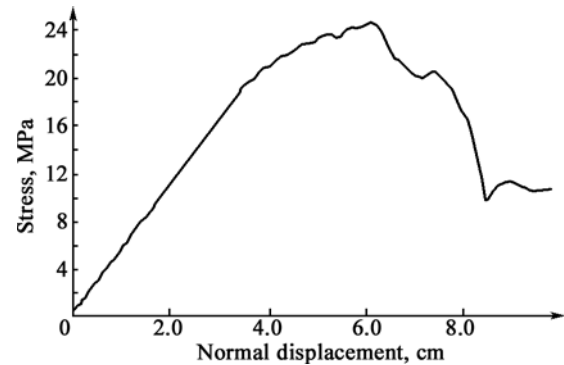


Figure 3. Complete stress-displacement curve of coal pillar at the depth of 215m

2.2.2. Failure characteristics of inclined strip coal pillar

In order to define the bearing capacity of a coal pillar depending on its occurrence depth and dip, the failure process of the coal pillar was simulated at different depth and dip. Initial and boundary conditions were taken as the same when simulating the vertical pillars.

According to the numerical simulation, the failure state of the coal pillar depends on its dip greatly. That is, the larger the dip of the pillar, the bigger the failed width of the pillar. The failure states of the pillars with different dips at the depth of 50m are shown in Fig 4.

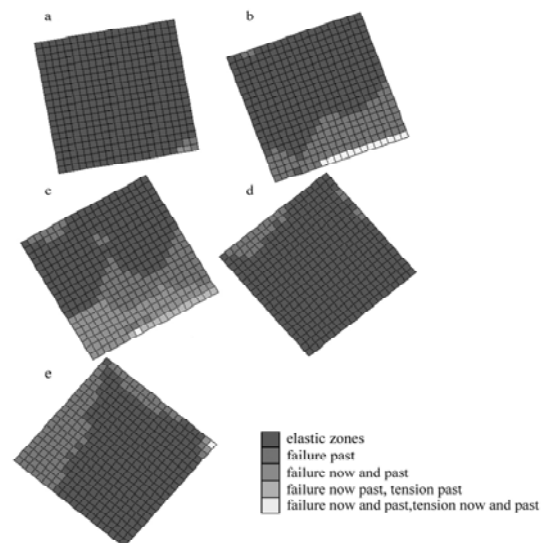


Figure 4. Failure state of coal pillar according to dip of pillar at the depth 50m

- a) in case of pillar with the angle of 10°, b) in case of pillar with 20°,
c) in case of pillar with 30°, d) in case of pillar with 40°,
e) in case of pillar with 50°

When the occurrence depth and the width of the pillar are the same, the dip makes a vast difference in the failure. The failure of the pillar starts from its bottom at the dip angle less than 30°, but from its roof at the dip angle larger than 30°.

In case that the pillar is not failed, its stress-strain relationship is the same as that shown in Fig. 5. For example, as for Fig. 4 a), the stress-strain curve of the pillar is shown in Fig. 5.

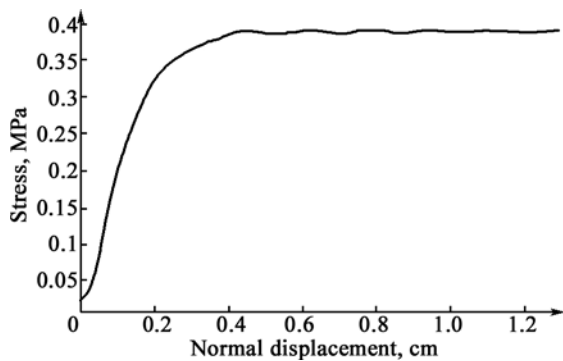


Figure 5. Stress–displacement relationship in the pillar without failure (when the depth of pillar is 50m and the dip of pillar is 10°)

On the other hand, when the pillar enters into the perfect plastic state, the stress–displacement relationship depends on the elasto–plastic strain softening model.

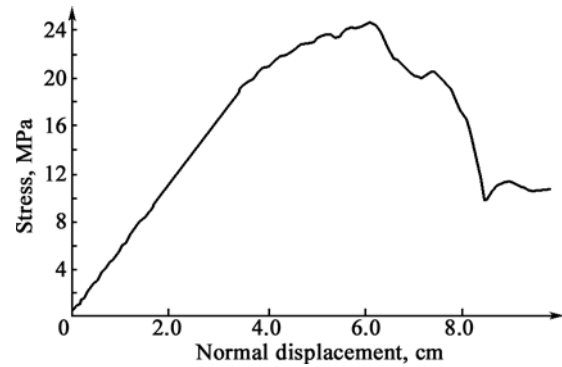


Figure 6. Complete stress–displacement curve of a coal pillar with the depth of 75m and the dip of 30°

When the coal pillar with various dips at different occurrence depths are failed, the residual strengths of the pillars depending on the lateral pressure are as follows in Table 2.

Table 2. Failure and residual strength of coal pillar at different depths and dips

No	Occurrence depth, m	Dip, °	Vertical rock Pressure, MPa	lateral rock pressure, MPa	Failure strength, MPa	Residual strength, MPa
1	50	10	1.25	0.4735	0.45	No failure
2	75	10	1.875	0.656	0.64	No failure
3	100	10	2.5	0.875	0.95	No failure
4	150	10	3.75	1.312 5	1.2	0.35
5	200	10	5	1.75	1.32	0.45
6	50	20	1.25	0.473 5	0.78	No failure
7	75	20	1.875	0.656	1.04	No failure
8	100	20	2.5	0.875	1.2	0.38
9	150	20	3.75	1.312 5	1.23	0.42
10	50	30	1.25	0.473 5	0.45	0.12
11	75	30	1.875	0.656	0.46	0.23
12	100	30	2.5	0.875	0.45	0.26
13	50	40	1.25	0.473 5	0.47	–
14	75	40	1.875	0.656	0.48	–
15	100	40	2.5	0.875	0.48	0.27
16	50	50	1.25	0.875	0.49	No failure
17	75	50	1.875	0.656	0.52	No failure
18	100	50	2.5	0.875	0.52	0.26

When comparing vertical pillars and inclined pillars in their failure state and bearing capacity, the inclined strip pillar has a failure tendency quite different from that of the vertical pillar and such characteristics should be taken into account. These were proved through the numerical simulation and field observation.

3. Comparison between research result to field observation

The analysis of field data observed from the relevant coal mine helped us know that coal pillars left in the goaves were all failed and rock formations on the mining panel were caved in the breaking arch type. The caving characteristics of the mining panel were observed through the prospecting adits driven at

intervals of 200m in the hanging wall of the coal seam as shown in Figure 7.

The 80m section of prospecting adit subsided to the depth of about 1.9m and such tendency appeared in every prospecting adit. The strike length of the subsided mining panel was about 2km. Caving has not developed yet on the ground surface.

This observation result shows that various kinds of coal pillars which have been left for roof control of the coal face and maintenance of entries have completely failed.

This result objectively confirms that the bearing capacity of the inclined strip coal pillar suggested in this paper is different from that of the vertical coal pillar and the bearing capacity of the strip coal pillar decreases and its failure width increases as the dip angle of the coal seam becomes large.

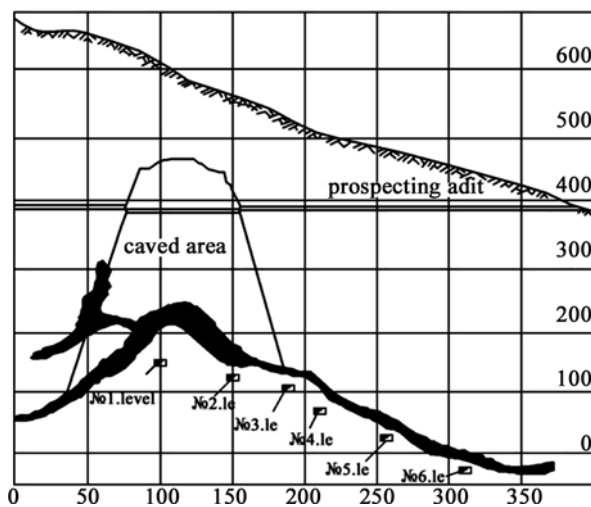


Figure 7. Sectional view of the mining panel caved in the 3rd gallery

4. Conclusion

The result of the numerical simulation that the strength of a coal pillar decreases and its failure width increases as its dip angle becomes large are in accord with the opinions in [4, 7, 12].

The vertical coal strip pillars in an anthracite coal mine start to fail from the depth of 215m, but inclined coal strip pillars start to fail from the depth of 50m and become completely failed at the depth of more than 70m. This was proved through the simulation and field observation. So we should take into account the bearing capacity of the coal pillar depending on the dip angle when designing inclined coal strip pillars.

Acknowledgements

The author is thankful to the technical staff and workers at the Ryong Dung Coal Mine and the Ryong Dung Coal Prospecting Corps under the Coal Industry Ministry of DPRK for their assistance in preparing the paper.

References

1. Ashok J., Shrivastva B.K., 2009, Numerical simulation of coal pillar strength, *Int. J. Rock Mech. Min. Sci.*, 46, 779–788.
2. Chen S. J., Guo W. J., 2014, Field investigation of long-term bearing capacity of strip coal pillars, *Int. J. Rock Mech. Min. Sci.*, 70, 109–114.
3. Gao W., 2014, Study on the width of the non-elastic zone in inclined coal pillar for strip mining, *Int. J. Rock Mech. Min. Sci.*, 72, 304–310.
4. Kush W. A., Banerjee G., 2005. Exploitation of developed coal mine pillars by shortwall mining—a case example, *Int. J. Rock Mech. Min. Sci.*, 42, 127–136.
5. Li X. B., Li D. U., 2013, Determination of the minimum thickness of crown pillar for safe exploitation of a subsea gold mine based on numerical modeling, *Int. J. Rock Mech. Min. Sci.*, 57, 42–56.
6. Murali M.G., Sheorey P.R., 2001. Numerical estimation of pillar strength in coal mines, *Int. J. Rock Mech. Min. Sci.*, 38, 1 185–1 192.
7. Poulsen B. A., Shen B., 2014, Strength reduction on saturation of coal and coal measures rocks with implications for coal pillar strength, *Int. J. Rock Mech. Min. Sci.*, 71, 41–52.
8. Poulsen B. A., 2010, Coal pillar load calculation by pressure arch theory and near field extraction ratio, *Int. J. Rock Mech. Min. Sci.*, 47, 1 158–1 165.
9. Please C. P., Mason D. P., 2013, Fracturing of an Euler–Bernoulli beam in coal mine pillar extraction, *Int. J. Rock Mech. Min. Sci.*, 64, 132–138.
10. Singh R. W., Singh S. K., 2012, Stability of the parting between coal pillar workings in level contiguous seams during depillaring, *Int. J. Rock Mech. Min. Sci.*, 55, 1–14.
11. Wang J. A., Shang X. C., 2008, Investigation of catastrophic ground collapse in Xingtai gypsum mines in China, *Int. J. Rock Mech. Min. Sci.*, 45, 1 480–1 499.
12. Wattimena K., Kramadibrata S., 2013, Developing coal pillar stability chart using logistic regression, *Int. J. Rock Mech. Min. Sci.*, 58, 55–60.